

influence of the d block, which favors eclipsing of the P-Fe-P plane, and an attractive cis interaction between H<sub>2</sub> and the adjacent Fe-H bond. Consequently, Fe(H<sub>2</sub>)(H)<sub>2</sub>(PEtPh<sub>2</sub>)<sub>3</sub> shows a broad minimum, and thus the maximum is necessarily lower: these competing factors tend to stabilize conformers even when away from their individual minima, thereby lowering the barrier due to either factor alone (in comparison to W(H<sub>2</sub>)(CO)<sub>3</sub>(PCy<sub>3</sub>)<sub>2</sub>).

**Acknowledgment.** This work was supported by the U.S. NSF and DOE, the French CNRS, and the European Economic Community. Work at Brookhaven was carried out under contract DE-AC02-76CH00016 with the U.S. Department of Energy, Office of Basic Energy Sciences. Work at Los Alamos was performed under the auspices of the U.S. Department of Energy, Division of Chemical Sciences, Office of Basic Energy Sciences. O.E. acknowledges the Indiana University Institute for Advanced

Study for a fellowship. The work has also benefited from the use of facilities at the Los Alamos Neutron Scattering Center, a national user facility funded as such by the Department of Energy, Office of Basic Energy Sciences. The Laboratoire de Chimie Théorique is associated with the CNRS (URA 506) and is a member of ICMO and IPCM. We thank Scott Horn of the Indiana University Molecular Structure Center and H. Blank of the Institut Laue-Langevin for skilled technical assistance, David Rathjen for his help during the neutron diffraction measurements, and Ilpo Mutikainen for valuable discussions.

**Supplementary Material Available:** Tables of full crystallographic details and anisotropic thermal parameters for FeL-(H)<sub>2</sub>(PEtPh<sub>2</sub>)<sub>3</sub>, where L = H<sub>2</sub> and N<sub>2</sub> (4 pages); listing of observed and calculated structure factors (77 pages). Ordering information is given on any current masthead page.

## Do Nonclassical Silabenzene Anions Exist? Synthesis and X-ray Crystal Structure of Crown Ether Stabilized Lithium Silacyclohexadienides, Li(12-crown-4)<sub>2</sub>Me<sub>2</sub>SiC<sub>5</sub>H<sub>5</sub> and Li(12-crown-4)<sub>2</sub>-*t*-Bu(H)SiC<sub>5</sub>H<sub>5</sub>

Peter Jutzi,<sup>\*,†</sup> Marion Meyer,<sup>†</sup> H. V. Rasika Dias,<sup>†</sup> and Philip P. Power<sup>†</sup>

Contribution from the Faculty of Chemistry, University of Bielefeld, 4800 Bielefeld, Universitätsstrasse, F.R.G., and Department of Chemistry, University of California, Davis, California 95616. Received December 4, 1989

**Abstract:** Metalation of 1,1-dimethyl-1-silacyclohexa-2,4-diene (**10**) and 1-*tert*-butyl-1-hydro-1-silacyclohexa-2,4-diene (**11**) with *n*-butyllithium leads to the corresponding silacyclohexadienyl lithium compounds, which on further treatment with the crown ether 12-crown-4 afford the deep red to violet crystalline title compounds [Li(12-crown-4)<sub>2</sub>][Me<sub>2</sub>SiC<sub>5</sub>H<sub>5</sub>] (**12**) and [Li(12-crown-4)<sub>2</sub>][*t*-Bu(H)SiC<sub>5</sub>H<sub>5</sub>] (**13**) as solvent-separated ion pairs with free silacyclohexadienide anions. The question whether the anions in **12** and **13** may be regarded as silicon-bridged pentadienide species or as nonclassical silabenzenes is answered on the basis of <sup>1</sup>H, <sup>13</sup>C, <sup>29</sup>Si NMR, and IR data of **10**–**13** and on the basis of an X-ray crystal structure determination of **12**. The π-bonding in these R<sub>2</sub>SiC<sub>5</sub>H<sub>5</sub><sup>-</sup> anions is found as quasiaromatic. In this context, the most intriguing structural and spectroscopic features are as follows: (I) planarity of the SiC<sub>5</sub> framework, short endocyclic silicon-carbon bonds, and rather long exocyclic Si-C bonds in **12**, (II) NMR signals for the ring-carbon hydrogens in **12** and **13** at comparatively low field, (III) dramatic low field shift in the <sup>1</sup>H NMR spectrum for the Si-H proton on going from **11** to **13**, and (IV) shift to lower wave numbers for the Si-H stretching mode (IR) and smaller Si-H coupling constant (<sup>29</sup>Si NMR) on going from **11** to **13**. The π-bonding in R<sub>2</sub>SiC<sub>5</sub>H<sub>5</sub><sup>-</sup> anions is qualitatively rationalized using the MO model (interaction of π-pentadienide with σ\*SiR<sub>2</sub> orbitals, negative hyperconjugation) and the valence bond approach (participation of the resonance structures **8c**, **8d**).

In phosphorus and sulfur chemistry, two different types of benzene-like heteroaromatic compounds have attracted widespread interest during the last 30 years. First, there are the classical (p-p)π systems with sp<sup>2</sup> hybridized heteroatoms such as the λ<sup>3</sup>-phosphabenzene **1**<sup>1</sup> and the isoelectronic thiapyrylium cations **2**.<sup>2</sup> The aromatic character of these compounds is now broadly accepted by both experimentalists and theoreticians. In contrast, the second group of compounds, the so-called nonclassical π systems involving four coordinate heteroatoms, has generated considerable controversy. Examples of these compounds include the λ<sup>3</sup>-phosphabenzene **3**<sup>3</sup> and the isoelectronic neutral thia-benzenes **4**.<sup>4</sup> The bonding discussion on these heterocyclic π systems has focused on the degree of participation by the heteroatom center in the delocalization through (p-d)π-overlap. Currently available experimental observations appear to rule out any bonding proposal [**3a**, **4a**] where appreciable π electron density is transferred from the carbon to the heteroatom in **3** and **4**. These

compounds are best described as cyclic phosphonium or sulfonium ylides, as indicated in **3b** and **4b**. The experimental results in favor of **3b** and **4b** mainly involve X-ray crystal structure investigations and NMR data.

Conjugative electron donation from a carbon p orbital to a sp<sup>3</sup> hybridized heteroatom cannot, in principle, be ruled out. In fact, recent publications have postulated that cyclic conjugation exists in the phosphirenium cation **5**<sup>5</sup> and in the phosphadiboretane **6**.<sup>6</sup>

(1) (a) Dimroth, K. *Fortschr. Chem. Forsch.* **1973**, *38*, 1. (b) Ashe, A. J., III; Sharp, R. R.; Tolon, J. W. *J. Am. Chem. Soc.* **1976**, *98*, 5451. (c) Ashe, A. J., III *Acc. Chem. Res.* **1978**, *11*.

(2) Yoneda, S.; Sugimoto, T.; Yoshida, Y. *Z. Tetrahedron* **1973**, *29*, 2009.

(3) Dimroth, K. *Acc. Chem. Res.* **1982**, *15*, 61.

(4) Maryanoff, B. E.; Stackhouse, I.; Senkler, G. H., Jr.; Mislow, K. *J. Am. Chem. Soc.* **1975**, 2718.

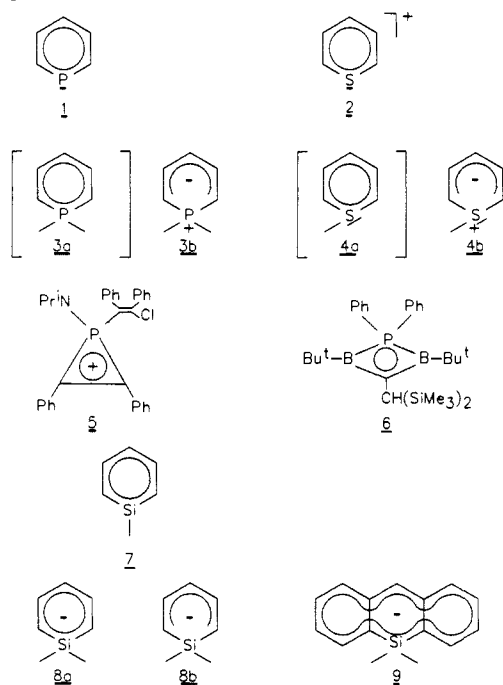
(5) Vural, J. M.; Weissmann, A.; Baxter, S. G.; Cowley, A. H.; Nunn, C. M. *J. Chem. Soc., Chem. Commun.* **1988**, 462.

(6) Berndt, A.; Klusik, H.; Pucs, C.; Wehrmann, R.; Meyer, H.; Lippold, U.; Schmidt-Lukasch, G.; Hunold, R.; Baum, G.; Massa, U. *Boron Chemistry; Proceedings of the 6th International Meeting on Boron Chemistry (IME-BORON)*, Hermanek, S., Ed.; World Scientific Press.

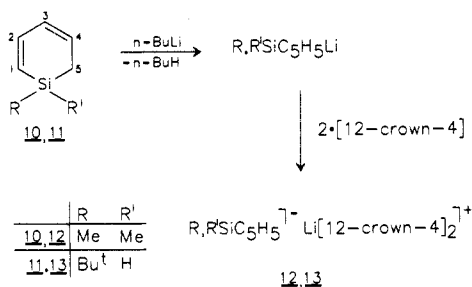
<sup>†</sup>University of Bielefeld.

<sup>†</sup>University of California.

## Scheme I



## Scheme II



Silicon analogues of the species 1–4 are also possible. For example, the heterocycles 7 and 8 are isoelectronic to the aromatic species 1, 2, and to 3, 4. The aromatic character of silabenzene,  $\text{SiC}_5\text{H}_6$ , has been proved unequivocally by PE spectroscopy and UV-vis absorption data.<sup>7</sup> This compound is stable only in an argon matrix at ca. 10 K, although bulky ligands can kinetically stabilize silabenzene.<sup>8</sup> However, species of type 8, which can be regarded as nonclassical silabenzene anions **8a** or as cyclic sili-con-bridged pentadienides **8b**, have not, to our knowledge, been investigated experimentally.

A related dibenzo derivative of 8, the 9-silaanthracene anion **9**, was synthesized and characterized by NMR and IR spectroscopy a number of years ago.<sup>9</sup> The anion was described as an aromatic species with carbon–silicon (p–d) $\pi$  bonding. Recent theoretical arguments questioned the use of d-orbitals by silicon or related elements in these or similar situations.<sup>10</sup>

In our recent work on silacyclohexadiene systems,<sup>11</sup> we also turned our attention to the question of bonding in so-called nonclassical sila-aromatic compounds. In this paper we describe the synthesis of crown ether complexes of lithium silacyclopentadienides and discuss the bonding on the basis of X-ray crystal structure, NMR, and IR investigations.

Table I. Crystallographic Data for **12**

formula	$\text{C}_{23}\text{H}_{43}\text{O}_3\text{SiLi}$
mol wt	482.69
color and habit	dark red-purple plates
crystal system	monoclinic
space group	$P2_1/n$
<i>a</i> , Å	12.186 (4)
<i>b</i> , Å	15.080 (8)
<i>c</i> , Å	15.139 (5)
$\beta$ , deg	109.66 (2)
<i>T</i> , K	130
<i>Z</i>	4
cryst dimens, mm	$0.95 \times 0.28 \times 0.025$
<i>d</i> (calcd), $\text{g cm}^{-3}$	1.22
radiation, (Å)	0.71069
$\mu(\text{Mo}, \text{K}\alpha)$ , $\text{cm}^{-1}$	1.26
range of transmsn fctrs	1.00–1.18
scan method, bkd offset	$\omega$ , 1.0, 1.0
scan speed, $\text{deg min}^{-1}$	60
$2\theta$ range, deg	0–52
octants collcd.	+ <i>h</i> , + <i>k</i> , + <i>l</i>
no. of data collcd.	5694
no. of unique data	5160
no. of data used in rfnmt	2726 ( $I > 2\sigma(I)$ )
no. of parameters rfnmt	304
<i>R</i> ( <i>F</i> )	0.072
<i>R</i> <sub>w</sub> ( <i>F</i> )	0.067
weighting scheme 1/ <i>w</i>	$[\sigma^2(F_o) + 0.00017F_o^2]$

**Synthesis of  $\text{Li}(\text{12-crown-4})_2\text{Me}_2\text{SiC}_5\text{H}_5$  (**12**) and  $\text{Li}(\text{12-crown-4})_2t\text{-Bu}(\text{H})\text{SiC}_5\text{H}_5$  (**13**).** According to Scheme II, 1,1-dimethyl-1-silacyclohexa-2,4-diene (**10**)<sup>12</sup> and 1-*tert*-butyl-1-hydro-1-silacyclohexa-2,4-diene (**11**),<sup>11a</sup> respectively, were metallated with *n*-butyllithium in tetrahydrofuran to afford the corresponding silacyclohexadienyllithium species, which are deep red in solution. Addition of 2 equiv of 12-crown-4 led to the crown ether complexes **12** and **13**. By crystallization from concentrated tetrahydrofuran solutions, the compounds **12** and **13** can be obtained as deep red to violet plates. The crystals are highly air- and moisture-sensitive and have to be kept at low temperatures (below 0 °C) to avoid thermal decomposition. The compounds **12** and **13** are characterized by NMR and IR spectroscopy and by elemental analyses (see Experimental Section).

The lithium cation in **12** and **13** is complexed by two crown ether molecules. This complexation affords solvent-separated ion pairs with free silacyclohexadienide anions which are present both in solution and in the solid state.

**<sup>1</sup>H, <sup>13</sup>C, <sup>29</sup>Si NMR, and IR Data of **12** and **13**.** The NMR spectra of **12** and **13** were recorded in  $\text{C}_6\text{D}_6$  solution. The signals for the crown ether hydrogen and carbon atoms are separated from those of the silacyclohexadienyl rings, so that assignments may be readily made. The numbering scheme for the ring protons and carbons is indicated in Scheme II.

The <sup>1</sup>H spectrum of **12** shows signals for H(1) and H(5) as a doublet of doublets centered at  $\delta = 4.68$  ( $J_{12} = 12.7$  Hz;  $J_{13} = 1.0$  Hz), for H(3) as a triplet of triplets at  $\delta = 4.95$  ( $J_{23} = 7.1$  Hz,  $J_{13} = 1.0$  Hz), for H(2) and H(4) as a doublet of doublets at  $\delta = 7.40$ , and for the methyl hydrogens as a singlet at  $\delta = 0.62$ . Similarly, the spectrum of **13** shows signals at  $\delta = 4.76$  (dd), 4.98 (tt), and 7.51 (dd), for H(1)/H(5), H(3), and H(2)/H(4) with  $J_{12} = 12.7$  Hz,  $J_{23} = 7.1$  Hz, and  $J_{13} = 1.0$  Hz. The *tert*-butyl hydrogens resonate at  $\delta = 1.36$ , whereas the SiH signal is found far downfield at  $\delta = 5.77$ . No coupling is observed between the hydrogen atom at silicon and the hydrogens at the neighboring carbon. On the basis of the Karplus equation, this indicates a torsion angle of 0° and an orientation of the  $\text{SiR}_2$  group perpendicular to the pentadienyl plane.

In the <sup>13</sup>C NMR spectrum of **12** the C(1)/C(5) carbon atoms have a chemical shift value of  $\delta = 86.4$ , the C(3) carbon atom appears at  $\delta = 91.0$ , and the C(2)/C(4) carbon atoms are found at  $\delta = 141.0$ . The  $\text{SiMe}_2$  carbon resonance is observed at  $\delta =$

(7) Souluiki, B.; Rosmus, P.; Bock, H.; Maier, G. *Angew. Chem.* **1980**, *92*, 56.

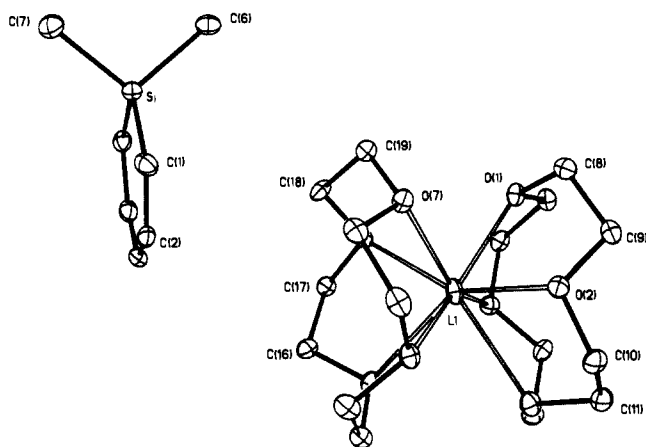
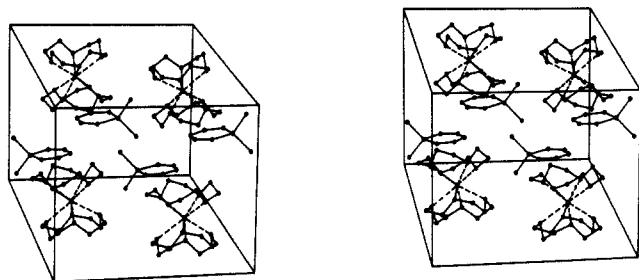
(8) (a) Märkl, G.; Schlosser, W. *Angew. Chem.* **1988**, *100*, 1009. *Angew. Chem., Int. Ed. Engl.* **1988**, *27*, 963. (b) Jutzi, P.; Meyer, M.; Reisenauer, H. P.; Maier, G. *Chem. Ber.* **1989**, *122*, 1227.

(9) Jutzi, P. *J. Organomet. Chem.* **1970**, *22*, 297.

(10) Janoschek, R. *Chem. Unserer Zeit* **1988**, *21*, 128.

(11) (a) Jutzi, P.; Otto, C.; Wippermann, T. *Chem. Ber.* **1984**, *117*, 1895. (b) Jutzi, P.; Meyer, M. *Chem. Ber.* **1988**, *121*, 1393.

(12) Chernychev, E. A.; Komalenkova, N. G.; Bashkirova, S. A.; Kisin, A. V.; Smirnova, F. M.; Mironov, V. A. *Zh. Oshch. Chim.* **1979**, *44*, 226.

Figure 1. Solid-state structure of **12**.Figure 2. Stereoscopic view of the unit cell of **12**.

9.2. Similarly, the signal for the carbon atoms C(1)/C(5), C(3), and C(2)/C(4) in **13** appear at  $\delta = 81.5, 92.4,$  and  $142.6$ . The Si-*t*-Bu group signals are observed at  $\delta = 20.1$  and  $27.1$ .

In the  $^{29}\text{Si}$  NMR spectra of **12** and **13**, resonances appear at  $\delta = -23.8$  and  $-16.2$ . These values are similar to those observed for the silacyclohexadienes **10** ( $-15.4^{30}$ ) and **11** ( $-19.3^{11a}$ ). In **13**, the Si-H coupling constant is rather small ( $J = 150$  Hz) compared to the values of **11** (191 Hz) and other alkylsilanes (190–210 Hz, *vide infra*). It is known from the literature<sup>13</sup> that  $^{29}\text{Si}$ - $^1\text{H}$  coupling constants can be correlated with Si-H stretching frequencies. Both these provide information on the electron density at the relevant silicon atom. In the IR spectrum of **13**, the Si-H stretching frequency is found at  $2020\text{ cm}^{-1}$ , whereas it appears at  $2114\text{ cm}^{-1}$  in the precursor molecule **11**.<sup>11b</sup>

**X-ray Crystal Structure Description of 12.** Crystallographic data for **12** are presented in Table I, atomic coordinates ( $\times 10^4$ ) and isotropic thermal parameters ( $\text{\AA}^2 \times 10^3$ ) in Table II, and selected bond distances ( $\text{\AA}$ ) and angles (deg) in Table III. The solid-state structure of **12** consists of well-separated, noninteracting solvated lithium cations  $[\text{Li}(12\text{-crown-}4)_2]^+$  and free silacyclohexadienide anions  $\text{Me}_2\text{SiC}_5\text{H}_5^-$ , as portrayed in Figure 1 and in a stereoscopic view of the unit cell in Figure 2. The lithium atom is coordinated, sandwich-like by two crown ether molecules. This geometry implies a coordination number of eight with average Li-O distances of  $2.37\text{ \AA}$ . Comparable arrangements are found for the lithium 12-crown-4 cations in compounds with free  $\text{CuR}_2^-$  and  $\text{PPh}_2^-$  counter anions.<sup>14,15</sup>

The  $\text{SiC}_5$  framework of the silacyclohexadienide anion is nearly planar; the dihedral angle between the planes C(1)SiC(5) and C(5)C(4)C(3)C(2)C(1) is  $0.8^\circ$ . The carbon-carbon bond lengths C(1)-C(2) and C(4)-C(5) are ca.  $1.37\text{ \AA}$  and ca.  $1.40\text{ \AA}$  for C(2)-C(3) and C(3)-C(4). The distance between the silicon atom and the ring carbon atoms C(1) and C(5) is  $1.83\text{ \AA}$ , which is rather short for a silicon atom bonded to a  $\text{sp}^2$  carbon atom [for comparison Si-C in  $\text{H}_3\text{SiCH}=\text{CH}_2$ :  $1.853\text{ \AA}$ ].<sup>16</sup> On the other hand,

Table II. Atomic Coordinates ( $\times 10^4$ ) and Isotropic Thermal Parameters ( $\text{\AA}^2 \times 10^3$ ) for **12**

	<i>x</i>	<i>y</i>	<i>z</i>	$U^m$
Si	2284 (1)	9130 (1)	1160 (1)	24 (1)
C(1)	3167 (5)	8404 (3)	2101 (3)	31 (2)
C(2)	3094 (5)	7496 (3)	2031 (4)	34 (2)
C(3)	2395 (5)	7011 (3)	1255 (4)	39 (2)
C(4)	1651 (5)	7421 (3)	441 (4)	35 (2)
C(5)	1469 (4)	8315 (3)	289 (3)	27 (2)
C(6)	3132 (5)	9904 (3)	645 (3)	29 (2)
C(7)	1375 (5)	9939 (3)	1575 (4)	38 (2)
Li	7341 (8)	6779 (5)	1235 (5)	25 (3)
O(1)	7859 (3)	7864 (2)	413 (2)	23 (1)
O(2)	9229 (3)	7150 (2)	2092 (2)	28 (1)
O(3)	8649 (3)	5439 (2)	1411 (2)	31 (1)
O(4)	7241 (3)	6183 (2)	-258 (2)	25 (1)
O(5)	6056 (3)	5522 (2)	1198 (2)	24 (1)
O(6)	5451 (3)	7168 (2)	339 (2)	23 (1)
O(7)	6844 (3)	8057 (2)	1902 (2)	26 (1)
O(8)	7431 (3)	6419 (2)	2744 (2)	26 (1)
C(8)	8826 (4)	8348 (3)	1027 (3)	29 (2)
C(9)	9757 (4)	7723 (3)	1598 (3)	32 (2)
C(10)	9952 (4)	6403 (3)	2503 (3)	29 (2)
C(11)	9845 (4)	5690 (3)	1789 (3)	33 (2)
C(12)	8351 (5)	4975 (3)	545 (3)	30 (2)
C(13)	8147 (4)	5590 (3)	-271 (3)	26 (2)
C(14)	7099 (4)	6920 (3)	-883 (3)	25 (2)
C(15)	8000 (4)	7622 (3)	-459 (3)	26 (2)
C(16)	4871 (4)	6809 (3)	886 (3)	27 (2)
C(17)	4699 (4)	6417 (3)	67 (3)	23 (2)
C(18)	4950 (4)	7874 (3)	708 (3)	27 (2)
C(19)	5921 (4)	8502 (3)	1209 (3)	27 (2)
C(20)	6629 (4)	7878 (3)	2750 (3)	28 (2)
C(21)	7521 (4)	7214 (3)	3278 (3)	29 (2)
C(22)	6616 (4)	5795 (3)	2870 (3)	32 (2)
C(23)	6415 (4)	5122 (3)	2102 (3)	27 (2)

<sup>a</sup>Equivalent isotropic  $U$  defined as one-third of the trace of the orthogonalized  $U_{ij}$  tensor.

Table III. Selected Distances ( $\text{\AA}$ ) and Angles (deg) for **12**

Si-C(1)	1.832 (5)	O(4)-C(13)	1.425 (6)
Si-C(6)	1.893 (6)	Si-C(5)	1.831 (4)
C(1)-C(2)	1.374 (7)	Si-C(7)	1.891 (6)
C(3)-C(4)	1.405 (7)	C(2)-C(3)	1.402 (7)
Li-O(1)	2.271 (9)	C(4)-C(5)	1.374 (6)
Li-O(3)	2.531 (9)	Li-O(2)	2.299 (9)
Li-O(5)	2.447 (9)	Li-O(4)	2.397 (9)
Li-O(7)	2.348 (9)	Li-O(6)	2.321 (8)
O(1)-C(8)	1.431 (5)	Li-O(8)	2.314 (9)
O(2)-C(9)	1.430 (6)		
C(1)-Si-C(5)	101.2 (2)	C(6)-Si-C(7)	101.6 (2)
C(5)-Si-C(6)	110.8 (2)	C(1)-C(2)-C(3)	126.2 (4)
C(5)-Si-C(7)	115.8 (2)	C(3)-C(4)-C(5)	126.8 (4)
Si-C(1)-C(2)	121.9 (3)	O(1)-Li-O(2)	74.0 (3)
C(2)-C(3)-C(4)	122.4 (4)	O(2)-Li-O(3)	70.1 (3)
Si-C(5)-C(6)	121.3 (3)	O(2)-Li-O(4)	110.3 (4)
O(1)-Li-O(3)	110.6 (4)	Li-O(1)-C(8)	109.3 (3)
O(1)-Li-O(4)	71.8 (3)	C(8)-O(1)-C(15)	113.6 (4)
O(3)-Li-O(4)	68.3 (2)	Li-O(2)-C(10)	113.9 (3)
Li-O(1)-C(15)	117.6 (3)	Li-O(3)-C(11)	110.7 (3)
Li-O(2)-C(9)	113.2 (3)	C(11)-O(3)-C(12)	114.2 (4)
C(9)-O(2)-C(10)	112.5 (4)	Li-O(4)-C(14)	106.8 (3)
Li-O(3)-C(12)	109.8 (3)	O(1)-C(8)-C(9)	110.6 (3)
Li-O(4)-C(13)	117.0 (3)	O(2)-C(10)-C(11)	110.9 (3)
C(13)-O(4)-C(14)	113.6 (4)	O(3)-C(12)-C(13)	112.1 (4)
O(2)-C(9)-C(8)	107.1 (4)	O(4)-C(14)-C(15)	110.8 (3)
O(3)-C(11)-C(10)	107.9 (4)	O(4)-C(13)-C(12)	107.0 (4)
C(1)-Si-C(6)	115.4 (2)	O(1)-C(15)-C(14)	105.9 (4)
C(1)-Si-C(7)	112.5 (2)		

the silicon-carbon (methyl) distances are about  $1.89\text{ \AA}$  and thus rather long for a silicon- $\text{sp}^3$  carbon bond [for comparison: the Si-C bond in  $\text{H}_3\text{SiCH}_3$  is  $1.867\text{ \AA}$ ,<sup>16</sup> and in tetraalkylsilanes it is  $1.870$ ].<sup>17</sup> Within the  $\text{SiC}_5$  ring, the angle at silicon is  $101.2^\circ$ .

(13) Bürger, H.; Kilian, W. *J. Organomet. Chem.* **1969**, *18*, 299.

(14) Hope, H.; Olmstead, M. M.; Power, P. P.; Xu, X. *J. Am. Chem. Soc.* **1984**, *106*, 819.

(15) (a) Olmstead, M. M.; Power, P. P. *J. Am. Chem. Soc.* **1985**, *107*, 2174. (b) Power, P. P. *Acc. Chem. Res.* **1988**, *21*, 147.

(16) Bürger, H. *Angew. Chem.* **1973**, *85*, 519.

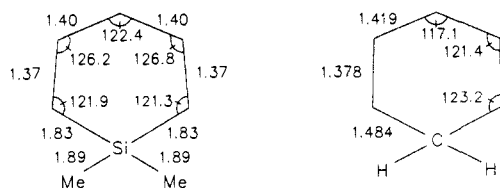


**Figure 3.** Bond distances (Å) and bond angles (deg) in the anions  $\text{Me}_2\text{SiC}_3\text{H}_5^-$  (X-ray) and  $\text{C}_6\text{H}_7^-$  (calcd<sup>21</sup>).

The angles between the  $\text{sp}^2$ -hybridized carbon atoms C(1)–C(5) are in the range of 121–127°. Thus, the rather small CSiC angle renders possible only small deviations from an ideal angle of 120° at the carbon atoms in the U-shaped pentadienide unit. The plane of the  $\text{SiMe}_2$  group is perpendicular to the  $\text{SiC}_3$  plane. The angle between the silicon atom and the exocyclic carbon atoms of the methyl groups is 101.6° and is thus surprisingly small. Consequently, the angles C(1)SiC(6) and C(1)SiC(7) are greater than expected for a  $\text{sp}^3$  hybridized silicon atom.

### Discussion

The bonding in the anionic species of the type  $\text{R}_2\text{SiC}_3\text{H}_5^-$  [silicon-bridged pentadienide anions **8b** or nonclassical silabenzene anions **8a**] has to be considered in the light of the X-ray crystal structure of **12** and the NMR spectroscopic data of **12** and **13**. Furthermore, the IR stretching frequency of the Si–H mode in **13** functions as a probe for the bonding at silicon.

As pointed out by many authors, the question of aromaticity is not a simple one. Most compounds can be readily classified as either aromatic or nonaromatic, but borderline cases may also occur.<sup>18</sup> Many attempts have been made to define criteria for aromaticity. Currently, the most popular and widely accepted parameters rely on geometrical criteria and on magnetic phenomena.

Obviously, cyclic conjugation in aromatic compounds generally tends to minimize the differences in bond length between formal double and single bonds. The shortening of bonds, when they are included in putatively aromatic ring systems, has often been regarded as good evidence for aromaticity. Nevertheless, geometrical criteria have to be interpreted carefully, especially in heteroaromatic compounds. For example, very similar bond lengths were observed in the aromatic  $\lambda^3$ -phosphabenzene of type **1** and in the nonaromatic cyclic phosphonium ylides of type **3b**. Ionic attraction of a positively charged phosphorus atom and a negatively charged carbon from a pentadienyl anion may explain the P–C bond shortening in the latter case.<sup>19</sup>

Compounds are considered aromatic, when induced diamagnetic  $\pi$ -electron ring currents are maintained in the molecule. The physical manifestations of the ring current are usually measured by NMR spectroscopy. For example, the ring protons of aromatic molecules typically show low field chemical shift values in the <sup>1</sup>H NMR spectrum. In addition, <sup>13</sup>C NMR shifts provide a good measure of electron density distribution. However, the use of magnetic parameters as criteria for aromaticity has been questioned.<sup>20</sup>

**Geometrical Criteria.** In Figure 3, bond lengths and angles in the anion of **12** are compared with those values obtained by the MINDO/3 calculation for the completely optimized structure of the corresponding  $\text{CH}_2$ -bridged species  $\text{C}_6\text{H}_7^-$ .<sup>21</sup> The bond lengths within the  $\text{C}_3$  units are very similar in both ions. The differences in bond angles are caused by the different size of the bridging groups,  $\text{Me}_2\text{Si}$  and  $\text{CH}_2$ . On this basis, the nonaromatic penta-

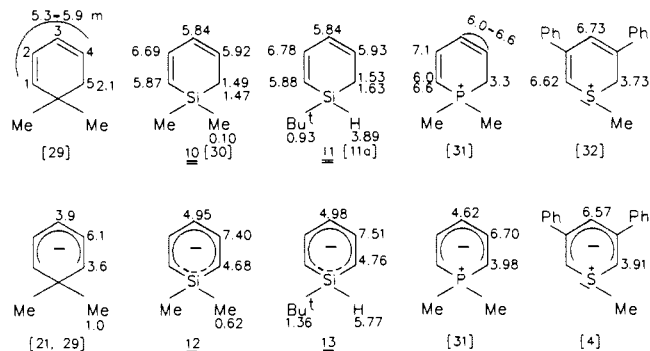


**Figure 4.** <sup>1</sup>H NMR data of (hetero)cyclohexadiene and -dienide systems, including **10**, **11**, **12**, and **13**.

dienide character postulated for  $\text{C}_6\text{H}_7^-$ <sup>21</sup> should also hold for the bonding in the  $\text{Me}_2\text{SiC}_3\text{H}_5^-$  anion.

However, an important feature of the anionic silicon-bridged structure is that the endocyclic silicon–carbon bond lengths are noticeably shorter than those in neutral Si–C( $\text{sp}^2$ ) systems. This indicates a higher Si–C bond order perhaps due to some degree of  $\pi$ -conjugation. Interestingly, the exocyclic silicon–carbon bonds are longer than expected for Si–C( $\text{sp}^3$ ) systems. The weakening of these bonds might be the result of  $\sigma^*$ -orbital population (vide infra).

The rather small exocyclic CSiC angle in **12** is also worthy of discussion. An angle of 101.6° indicates a higher p-character of the relevant bonding orbitals at silicon. This allows more s-character in the bonding to the ring-carbon atoms necessary for  $\pi$ -delocalization (vide infra). The planarity of the  $\text{SiC}_3$  framework in **12** enables electron delocalization from the pentadienide system onto the silicon center to occur. On the other hand, the planar  $\text{SiC}_3$  structure does not rule out nonaromaticity.

**Criteria from <sup>1</sup>H, <sup>13</sup>C, and <sup>29</sup>Si NMR Spectroscopy.** In Figure 4, the <sup>1</sup>H NMR data for the anions of **12** and **13** and for the corresponding precursor molecules, the silacyclohexadienes **10** and **11**, are portrayed together with <sup>1</sup>H NMR data for some cyclohexadiene and cyclohexadienyl species from carbon, phosphorus, and sulfur chemistry for comparison.

In the cyclohexadiene compounds of Figure 4 the olefinic protons are all in the expected region. Differences in the chemical shift of the allylic protons, which appear in the range 1.5–3.7 ppm, can be attributed to the influence of the corresponding heteroatom in the  $\alpha$ -position.

In the cyclohexadienide compounds, most of the <sup>1</sup>H NMR resonances for the relevant protons do not appear in the aromatic region [<sup>1</sup>H NMR of benzene  $\delta = 7.3$ ]. The marked upfield chemical shifts noted for most of the protons and the large chemical shift differences for protons at C(1), C(3), C(5) and at C(2), C(4) rule out aromaticity for most of these compounds. Consequently they may be characterized as cyclic pentadienide systems with no aromaticity. In contrast, a borderline case is observed for the anions of the silicon compounds **12** and **13**. Here, the protons at C(2), C(4) and also at C(1), C(3), C(5) show resonances at comparatively low field; thus, some degree of aromaticity and diamagnetic  $\pi$ -electron ring current can be postulated.

The most impressive support for a diamagnetic ring current in **13** stems from the proton resonance of the SiH group. Whereas in the neutral precursor molecule **11** the SiH resonance is observed at  $\sigma = 3.89$  ppm,<sup>11a</sup> it is shifted nearly 2 ppm downfield in the anion of **13**. Generally, a better shielding in the <sup>1</sup>H NMR spectrum is observed with increasing hydridic character of the Si–H bond. According to correlations found by Webster,<sup>22</sup> at least a small high field shift could have been expected on going from **11** to the anionic species **13**. Thus, ring current effects are probably responsible for the observed dramatic low field shift. The same argument has already been used in the discussion of the bonding in a 9-silaanthracene anion.<sup>9</sup> The changes in the values of the SiH coupling constants are discussed in the context with changes in the Si–H stretching frequencies (vide infra).

(17) *Special Publication, No. 18*; The Chemical Society: London, 1965; S.22s. *Molecular Structure and Dimensions*; Crystallographic Data Centre: Cambridge.

(18) (a) Katritzky, A. R.; Barczynski, P.; Musumarra, G.; Pisano, D.; Szafran, M. *J. Am. Chem. Soc.* **1989**, *111*, 7. (b) Binsch, G. *Naturwissenschaften* **1973**, *60*, 269. (c) Maier, G. *Chem. Unserer Zeit* **1975**, *9*, 131.

(19) Whangbo, M. W.; Wolfe, S.; Bernardi, F. *Can. J. Chem.* **1975**, *53*, 3040.

(20) Million, R. B. *Pure Appl. Chem.* **1980**, *52*, 1541.

(21) Olah, G. H.; Asensio, G.; Mayr, H.; Schleyer, P. v. R. *J. Am. Chem. Soc.* **1978**, *100*, 4347.

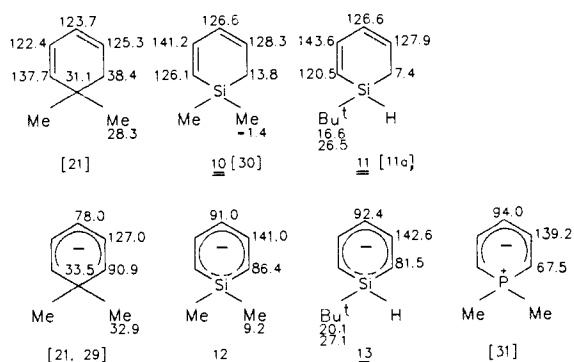


**Figure 5.**  $^{13}\text{C}$  NMR data of (hetero)cyclohexadiene and -dienide systems, including **10**, **11**, **12**, and **13**.

$^{13}\text{C}$  NMR shifts generally provide the best measure of electron density distribution in  $\pi$ -systems. In Figure 5, the  $^{13}\text{C}$  NMR data for the anions in **12** and **13** and for their precursors **10** and **11** are collected together with data for some other cyclic diene and dienide compounds useful for comparison. The most striking feature of the data for all the cyclohexadienide systems, independent of the bridging units  $[\text{CR}_2, \text{SiR}_2, \text{PR}_2^+]$ , is that the odd-numbered carbons all appear at higher field (67–94 ppm) than the even-numbered carbons (127–143 ppm). Thus the ring-carbon atoms C(1), C(3), C(5) bear a high electron density as expected for pentadienide structures.

The total upfield shift for C(1) to C(5) in  $\text{Me}_2\text{C}_5\text{H}_5^-$  relative to benzene ( $\delta = 128.7$  ppm) is 129.7 ppm, approximately that expected for the location of one additional electron on the five  $\text{sp}^2$ -hybridized ring-carbon atoms.<sup>21</sup> Similarly, the total upfield shift in  $\text{Me}_2\text{PC}_5\text{H}_5$  is 135.7 ppm, which is in the same range as in the  $\text{Me}_2\text{C}$ -bridged compound. Interestingly, the total upfield shifts in the  $\text{R}_2\text{Si}$ -bridged species in **12** and **13** are only 97.7 and 102.9 ppm, respectively. This indicates the location of less than one additional electron on the five ring carbons and thus a partial electron delocalization to the bridging  $\text{R}_2\text{Si}$  groups. However, caution has to be exercised not to overestimate the values of these empirical calculations;  $^{13}\text{C}$  shieldings are not solely determined by  $\pi$ -charge densities.<sup>21,23</sup> The  $^{13}\text{C}$  NMR data of the precursor molecules  $\text{Me}_2\text{CC}_5\text{H}_6$ ,  $\text{Me}_2\text{SiC}_5\text{H}_6$  (**10**), and  $t\text{-Bu(H)SiC}_5\text{H}_6$  (**11**) are in the expected range for vinylic and allylic carbon atoms and need no further discussion.

**Si-H Stretching Frequencies and Coupling Constants as Criteria.** The Si-H stretching frequency is a reliable probe of the polarity and thus the electron-density distribution in the Si-H bond. Absorption at high wavenumbers is observed for compounds with a protic hydrogen (e.g.,  $\nu$  SiH in  $\text{HSiF}_3$ : 2200  $\text{cm}^{-1}$ <sup>24</sup>), whereas compounds with a hydridic hydrogen absorb at lower wavenumbers (e.g.,  $\nu$  SiH in  $\text{KSiH}_3$ : 1880  $\text{cm}^{-1}$ <sup>24</sup>). A shift of about 100  $\text{cm}^{-1}$  to lower wavenumbers on going from the neutral Si-H compound **11** to the anionic species in **13** indicates transfer of electron density into the Si-H bond.

According to the investigations of Bürger,<sup>13</sup> the Si-H stretching frequency can be correlated with the corresponding coupling constant  $J(\text{SiH})$ . Absorption at lower wavenumbers corresponds to smaller coupling constants (e.g.,  $J(\text{SiH})$  in  $\text{HSiF}_3$ , 388 Hz; in  $\text{KSiH}_3$ , 75 Hz).<sup>25</sup> In accord with this correlation,  $J(\text{SiH}) = 191$  Hz in **11** is reduced to  $J(\text{SiH}) = 150$  Hz in **13**.

Furthermore, values of SiH coupling constants can be correlated with the hybridization at silicon in the relevant Si-H bond. Generally, lower  $J$  values correspond to higher p-character. In the case of **11** and **13**, the  $J(\text{SiH})$  values indicate more p-character in the Si-H bond of **13** and thus more s-character in the remaining

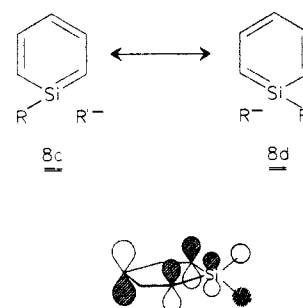


**Figure 6.** Representation of the HOMO in a nonclassical silabenzene anion and corresponding description in the valence-bond picture by the resonance structures **8c** and **8d**.

Si-C(ring) bonds consistent with some  $\pi$ -electron delocalization.

### Summary

On the basis of NMR, IR, and X-ray crystal structure data, the  $\pi$ -bonding picture in  $\text{R}_2\text{SiC}_5\text{H}_5^-$  anions may be described as quasi-aromatic. Arguments for a nonaromatic  $\text{R}_2\text{Si}$ -bridged pentadienide structure **8b** as well as for some degree of  $\pi$ -electron delocalization in a nonclassical silabenzene anion **8a** can be presented.

$\pi$ -Electron delocalization across the silicon atom in **12** or **13** can occur by using the vacant antibonding ( $\sigma^*$ ) orbitals of the  $\text{SiR}_2$  group (alternative description:  $\pi^*\text{SiR}_2$ ). In Figure 6 the relevant molecular orbital of  $\pi$ -symmetry is portrayed, resulting from a linear combination of a pentadienide HOMO and the  $\sigma^*\text{SiR}_2$  orbitals. The electron delocalization to the silicon atom leads to a strengthening of the Si-C(ring) bonds due to some double bond character and to a weakening of the Si-R  $\sigma$  bonds. This situation corresponds to a "negative hyperconjugation" effect<sup>26</sup> and can be expressed in the valence-bond picture by the resonance structures **8c** and **8d** in Figure 6.

Similar arguments have been presented by Olah<sup>21</sup> on the basis of MINDO/3 calculations for the justification of a rather poor electron delocalization in the cyclohexadienide system: the  $\pi$ -electron density of a pentadienide fragment decreases only by 0.14 electrons due to interaction with a methylene group. Generally, a  $\sigma^*\text{CR}_2$  orbital is higher in energy than the comparable  $\sigma^*\text{SiR}_2$  orbital and thus less suitable for a stabilizing interaction. On the basis of these qualitative molecular orbital arguments, the more pronounced  $\pi$ -electron delocalization in silacyclohexadienide systems can easily be explained.

### Experimental Section

**Bis(12-crown-4)lithium 1,1-Dimethyl-1-silacyclohexadienide (12).** A 4.00 mM solution of *n*-butyllithium in hexane was added dropwise to a solution of 4.97 mg (4.00 mmol) of **10** in 25 mL of tetrahydrofuran. After 5 h, 1.41 g (8.00 mmol) of 12-crown-4 was added to the deep-red solution. The resultant violet solution was concentrated to ca. 10 mL. On cooling, the complex **12** crystallizes in the form of deep red violet platelets, which are extremely air- and moisture-sensitive: yield 1.08 g (57%); mp 86–90 °C;  $^1\text{H}$  NMR ( $\text{C}_6\text{D}_6$ ) 0.62 (s, 6 H,  $\text{SiMe}_2$ ), 3.37 (s, 32 H, 12-crown-4), 4.68 (dd,  $^3J_{1,2} 12, 7$  Hz,  $^4J_{1,3} 1.1$  Hz, 2 H, H1/5), 4.95 (tt,  $^3J_{2,3} 7.1$  Hz, 1 H, H3), 7.40 (dd, 2 H, H2/4);  $^{13}\text{C}$  NMR ( $\text{C}_6\text{D}_6$ ) 9.2 ( $\text{SiMe}_2$ ), 67.6 (12-crown-4), 86.4 (C1/5), 91.0 (C4), 141.0 (C2/4);  $^{29}\text{Si}$  NMR ( $\text{C}_6\text{D}_6$ ) -23.8.  $\text{C}_{23}\text{H}_{43}\text{LiO}_8\text{Si}$  (482.6). Anal. Calcd: C, 57.24; H, 8.98. Found: C, 56.78; H, 8.98.

**Bis(12-crown-4)lithium 1-tert-Butyl-1-hydro-1-silacyclohexadienide (13).** The synthetic procedure was analogous to that of **12**; 6.09 mg (4.00 mmol) of **11**, 4.00 mmol of *n*-butyllithium, 1.41 g (8.00 mmol) of 12-crown-4 were used. **13** was obtained in the form of violet, extremely air- and moisture-sensitive, crystals: yield 0.98 g (49%), melting point 110–111 °C;  $^1\text{H}$  NMR ( $\text{C}_6\text{D}_6$ ) 1.36 (s, 9 H,  $\text{CMe}_3$ ), 3.37 (s, 32 H, 12-crown-4), 4.76 (dd,  $^3J_{1,2} = 12.7$  Hz,  $^4J_{1,3} = 1.0$  Hz, 2 H, H1/5), 4.98 (tt,  $^3J_{2,3} 7.1$  Hz, 1 H, H3), 5.77 (s, 1 H, SiH), 7.51 (dd, 2 H, H2/4);  $^{13}\text{C}$  NMR ( $\text{C}_6\text{D}_6$ ) 20.1 ( $\text{CMe}_3$ ), 27.1 ( $\text{CMe}_3$ ), 68.3 (12-crown-4), 81.5 (C1/5), 92.4 (C3), 142.6 (C2/4);  $^{29}\text{Si}$  NMR ( $\text{C}_6\text{D}_6$ ) -16.2 (d,  $J(\text{SiH}) = 150$  Hz); IR (toluene) 2020  $\text{cm}^{-1}$ ,  $\nu$  Si-H.  $\text{C}_{25}\text{H}_{47}\text{LiO}_8\text{Si}$  (510.7). Anal. Calcd: C, 58.80; H, 9.28. Found: C, 57.77; H, 9.10.

**X-ray Crystallographic Studies. Structure Determination and Refinement.** A suitable crystal was chosen and attached to a glass fiber with silicone grease and mounted in the cold stream of synchrotron P21 diffrac-

(22) Webster, D. E. *J. Chem. Soc.* **1960**, 5132.

(23) O'Brien, D. H.; Hart, A. J.; Russell, C. R. *J. Am. Chem. Soc.* **1975**, *97*, 4410.

(24) Bürger, H.; Eujen, R.; Marsmann, H. S. *Z. Naturforsch.* **1974**, *29b*, 149.

(25) Harris, R. K.; Kennedy, J. D.; McFarlane, W. In *NMR and the Periodic Table*; Academic Press: New York, 1978; p 309.

tometer equipped with a locally modified LT-1 low-temperature device. No decay in the intensity of standard reflections was observed during the data collection.

The structure was solved by direct methods in the space group  $P2_1/n$ . All computing was carried out by using SHELXTL Version 5 programs installed in a Data General Eclipse computer. Atomic scattering factors and anomalous dispersion corrections were from common sources.<sup>27</sup> An absorption correction was applied,<sup>28</sup> and the structure refinement pro-

ceeded smoothly. All non-hydrogen atoms were assigned anisotropic thermal parameters. Hydrogen atoms were refined by using a riding model in which an idealized C–H vector, 0.96 Å in length, was recalculated with each cycle of refinement. Isotropic hydrogen thermal parameters were fixed at 1.2 times the equivalent isotropic thermal parameter of the bonded atom.

Further details are in Table I. Atom coordinates are given in Table II. Selected bond distances and angles are given in Table III.

**Acknowledgment.** We thank the NATO Scientific Affairs Division for financial support; a scholarship from the "Studienstiftung des Deutschen Volkes" for M.M. is gratefully acknowledged.

**Supplementary Material Available:** Tables of bond distances and angles, anisotropic thermal parameters, and hydrogen coordinates (6 pages); listings of structure factor amplitudes (16 pages). Ordering information is given on any current masthead page.

(26) Farnham, W. B.; Dixon, D. A.; Calabrese, J. C. *J. Am. Chem. Soc.* **1988**, *110*, 2607.

(27) *International Tables for X-ray Crystallography*; Kynoch Press: Birmingham, England, 1976; Vol. IV.

(28) Program XABS was written by H. Hope and B. Moezzi. The program obtains an absorption tensor from  $F_o - F_c$  differences. Moezzi, B.; Ph.D. Dissertation, University of California, Davis, 1987.

(29) Di Mauro, P. T.; Wolczanski, P. T. *Organometallics* **1987**, *6*, 1947.

(30) Jutzi, P. Unpublished work.

(31) Ashe, A. J., III; Smith, T. W. *J. Am. Chem. Soc.* **1976**, *98*, 786.

(32) Hortmann, A. G.; Harris, R. L. *J. Am. Chem. Soc.* **1970**, *92*, 1803.

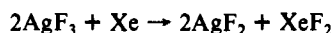
## Spontaneous Oxidation of Xenon to Xe(II) by Cationic Ag(II) in Anhydrous Hydrogen Fluoride Solutions

Boris Zemva,<sup>†</sup> Rika Hagiwara,<sup>‡</sup> William J. Casteel, Jr.,<sup>‡</sup> Karel Lutar,<sup>†</sup> Adolf Jesih,<sup>†</sup> and Neil Bartlett<sup>\*‡</sup>

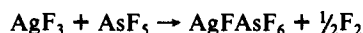
Contribution from the Materials and Chemical Sciences Division, Lawrence Berkeley Laboratory, and Department of Chemistry, University of California, Berkeley, California 94720, and "Jožef Stefan" Institute, "Edvard Kardelj" University, 61000 Ljubljana, Yugoslavia.  
Received January 3, 1990

**Abstract:** Blue solutions, prepared by dissolving  $\text{AgF}_2$  in anhydrous hydrogen fluoride (AHF) with  $\text{BF}_3$  or  $\text{AsF}_5$ , oxidize Xe, at  $\sim 20^\circ\text{C}$ , to produce nearly colorless solids. Overall reactions (all in AHF) are as follows:  $2\text{AgF}_2 + 2\text{BF}_3 + \text{Xe} \rightarrow \text{XeF}_2 + 2\text{AgBF}_4$ ;  $4\text{AgF}_2 + 5\text{AsF}_5 + 2\text{Xe} \rightarrow \text{Xe}_2\text{F}_3\text{AsF}_6 + 4\text{AgAsF}_6$ . Solid  $\text{AgF}_2$  does not interact, at  $\sim 20^\circ\text{C}$ , with Xe.  $\text{Ag(I)}$  in AHF is catalytic to the interaction of Xe with  $\text{F}_2$  ( $\text{Xe} + \text{F}_2 \rightarrow \text{XeF}_2$ ), but  $\text{XeF}_2$  precipitates  $\text{AgF}_2$  from  $\text{Ag(II)}$  AHF solutions (e.g.  $\text{AgFAsF}_6 + 2\text{XeF}_2 \rightarrow \text{Xe}_2\text{F}_3\text{AsF}_6 + \text{AgF}_2$ ). To maintain the  $\text{Ag(I/II)}$  catalyst the fluoride-ion donor,  $\text{XeF}_2$ , must be neutralized with acid, e.g.  $2\text{Xe} + 2\text{F}_2 + \text{AsF}_5 \rightarrow \text{Xe}_2\text{F}_3\text{AsF}_6$ .

A new approach to the synthesis of polymeric binary fluorides<sup>1</sup> has provided  $\text{AgF}_3$  as a diamagnetic red solid, isostructural with  $\text{AuF}_3$ . This fluoride<sup>2</sup> was found to oxidize xenon gas spontaneously at  $\sim 20^\circ\text{C}$  according to the equation



In liquid anhydrous hydrogen fluoride (AHF), together with the strong fluoride ion acceptor  $\text{AsF}_5$ , the  $\text{AgF}_3$  reacted to form a blue solution with elimination of  $\text{F}_2$ . From this solution the previously described  $\text{Ag(II)}$  salt,<sup>3</sup>  $\text{AgFAsF}_6$ , was isolated, the overall reaction being



When the oxidation of xenon was carried out with the  $\text{AgF}_3$ , in AHF, in the presence of  $\text{AsF}_5$ , it was observed that the silver was reduced to  $\text{Ag(I)}$  (i.e.  $\text{AgAsF}_6$ ). This implied that cationic  $\text{Ag(II)}$  species were capable of oxidizing xenon and, therefore, that  $\text{AgF}_2$ , in AHF, in the presence of strong fluoroacids should also do so. This has proved to be the case not only with  $\text{AgF}_2/\text{AHF}/\text{AsF}_5$  but also with  $\text{AgF}_2/\text{AHF}/\text{BF}_3$ . In addition  $\text{Ag(I/II)}$  in AHF has been shown to catalyze the combination of Xe with  $\text{F}_2$  in the presence of  $\text{AsF}_5$  to yield  $\text{Xe}_2\text{F}_3^+\text{AsF}_6^-$ .

### Results and Discussion

Although solid  $\text{AgF}_2$  does not oxidize xenon at ordinary temperatures and pressures, the blue solutions, prepared by the interaction of  $\text{AgF}_2$  with fluoride ion acceptors such as  $\text{AsF}_5$  or  $\text{BF}_3$  in AHF, quickly do so at  $\sim 20^\circ\text{C}$ . That the strongly oxidizing character of these blue solutions is associated with cationic  $\text{Ag(II)}$  is indicated by the structures of the deep blue solids,  $\text{AgFAsF}_6$ , and  $\text{Ag(SbF}_6)_2$  first prepared and described<sup>3,4</sup> by Gantar et al.

In the  $\text{AgFAsF}_6$  structure,<sup>3</sup> fluorine ligands symmetrically bridge the  $\text{Ag(II)}$  in  $(\text{AgF})_n^{n+}$  chains. It is probable that such chains also occur in the dark blue solid of composition  $\text{AgFBF}_4$  isolated in the course of this work (see Table I). Perhaps the AHF solutions, of these 1:1 compounds of  $\text{AgF}_2$  with fluoride ion acceptors, contain solvated  $\text{AgF}^+$  species. These 1:1 compounds are not highly soluble in AHF, however, and the interactions of these solutions with Xe are sluggish in comparison with the  $\text{Ag(II)}$  solutions obtained when additional  $\text{BF}_3$  or  $\text{AsF}_5$  is used. Two moles of fluoride ion acceptor to one mole of  $\text{Ag(II)}$  appears to be optimal. This stoichiometry suggests that the oxidizing species

(1) Žemva, B.; Lutar, K.; Jesih, A.; Casteel, W. J., Jr.; Bartlett, N. J. *Chem. Soc., Chem. Commun.* **1989**, 346.

(2) Žemva, B.; Lutar, K.; Jesih, A.; Wilkinson, A. P.; Cox, D. E.; Casteel, W. J., Jr.; Bartlett, N. To be published.

(3) Gantar, D.; Frleč, B.; Russell, D. R.; Holloway, J. H. *Acta Crystallogr.* **1987**, *C43*, 618.

<sup>†</sup> Institut Jožef Stefan, Ljubljana.

<sup>‡</sup> University of California.